COMPUTATIONAL MODELLING AND ANTIOXIDANT ACTIVITIES OF SUBSTITUTED N-(METHOXYSALICYLIDENE)ANILINES

ABSTRACT

The computational modelling and total antioxidants activities of three N-(methoxysalicylidene)anilines namely N- (methoxysalicylidene)aniline [**I**], N-(methoxysalicylidene)-4-chloroaniline [**II**] and N-(methoxysalicylidene)-5-chloro-2-methylaniline [**III**] were reported. The compounds were synthesized and characterized by elemental analysis, infrared, ultraviolet, proton and carbon-13 nuclear magnetic resonance. Quantum chemical computations were also performed on the optimized structures of the compounds using Density Functional Theory. The infrared, nuclear magnetic resonance and ultraviolet spectra of the compounds were calculated and the results likened to the equivalent experimental spectra to enhance the structural identification. The calculated infrared, nuclear magnetic resonance and ultraviolet spectra were comparable to the experimental spectra. The total antioxidant capacities of the Schiff bases were evaluated by phosphomolybdenum assay and the results indicated that all the synthesized compounds displayed antioxidant activities.

Keywords: N-(methoxysalicylidene)anilines, substituents, computational modelling, antioxidant activities.

1. INTRODUCTION

Schiff bases are compounds like ketone or aldehyde except that the carbonyl groups (C=O) are being replaced by imines or azomethines (HC=N) groups. They are the products of condensation reactions between primary amines and carbonyl compounds. They were discovered by a German chemist, Hugo Schiff in 1864 [1-4]. They can also be called imines or azomethines. The ensuing imines take part in bonding with metal ions through nitrogen lone pair electrons. The azomethine moieties are essential for biological activities. They are very useful active centres of many biological systems [5, 6]. They help to make clear the mechanism of transamination and racemization reactions in biological systems. The nitrogen atom of azomethines may partake in the formation of hydrogen bonds with the active centres of cell constituents and interfere in normal cell processes [7]. They act as excellent chelating ligands with broad range of properties, which can be changed by introducing numerous substituents on either the carbonyl or amine rings.

Schiff bases have attracted attention because of their broad range of biological activities. Many literatures have reported them to having anti-inflammatory [8], analgesic [9], antimicrobial [4],

anticonvulsant [10], antitubercular [11], anticancer [12], antioxidants [13], anthelmintic, antimalarial [14], antifungal and antitumour properties [15]. They are also used in the treatment of diabetes [16] and as model systems for biological macromolecules [17].

Although, many literatures have reported the synthesis and spectroscopic of different Schiff bases but reports on the antioxidants properties of these compounds are scanty. Thus, this study which investigated the computational modelling and total antioxidant activities of N-(methoxysalicylidene)anilines. Nowadays, with the advancement of computational methods, it is possible to reliably modelled and determine the molecular properties of different compounds which help augment experimental observations. Therefore, in order to correlate between the theoretical and experimental results, the molecular structures of the compounds were modelled and theoretical calculations using Density Functional Theory (DFT) were carried out on the optimized structures. These were employed for the UV-Visible, IR and NMR spectroscopies. A comparison of the resemblances between the theoretical and experimental results of the compounds could further be employed for structural identification.

2. MATERIAL AND METHODS

2.1 Reagents

Aniline, *p*-chloroaniline, 5-chloro-2-methylaniline and 2-hydroxy-5-methoxybenzaldehyde were purchased from Merck (Germany) and used as supplied. The solvent DMSO (dimethylsulfoxide) was of analytical grade and used without further purification while the ethanol was distilled.

2.2. Instruments

The elemental analyses were carried out on Finnigan Flash EA 1112 series. The electronic spectra were recorded on Shimadzu UV-2600 series (Japan), in DMSO. The infrared spectra were obtained using a Perkin-Elmer 400 FT-IR/FT-FIR. The NMR spectra were recorded on a Bruker Avance 111 600 in DMSO-D_6 solution with tetramethylsilane (TMS) as internal standard.

2.3 Synthesis of the Schiff bases

The Schiff bases were synthesized according to literature [18]. 0.015 mole of 2-hydroxy-5-methoxybenzaldehyde in 10 mL ethanol was added in drops to a stirring solution of 0.015 mole of the corresponding amine in 15 mL of ethanol. The resulting solution was stirred for 2 hours on addition of

three drops of methanoic acid. The coloured precipitates were filtered and washed with cold ethanol, recrystallized from ethanol and dried in a desiccator over silica gel for two days.

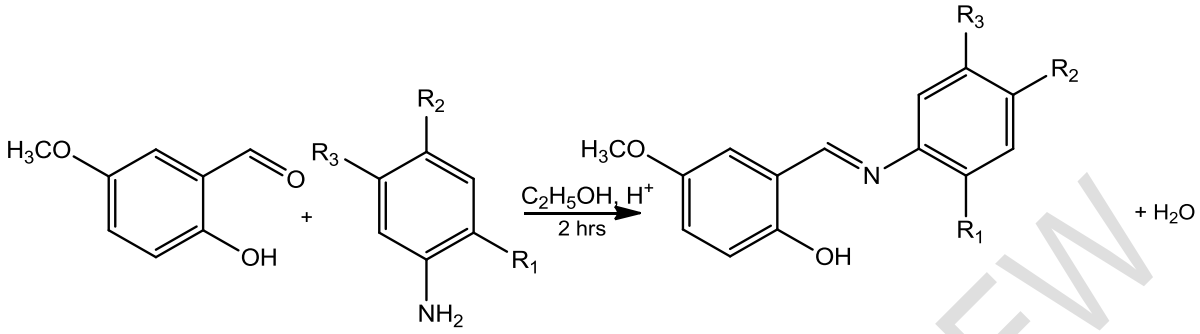

R_1= H, R_2= H, R_3= H (**I**); R_1= H, R_2= Cl, R_3= H (**II**); R_1= CH_3, R_2= H, R_3= Cl (**III**)

Scheme 1. Synthetic route to compounds (I-III).

2.4 Details of Computational Modelling

The Schiff bases were modelled and optimized using Gaussian 09 and Spartan '14 computational software packages. Density Functional Theory (DFT) was employed for the geometry optimization, chemical shifts, electronic transitions and frequency calculations of the compounds based on preliminary conformational search of the molecules with molecular mechanics force field. The DFT calculations were performed on the most stable conformer in the ground state using Becke's three-parameter hybrid functional employing the Lee-Yang-Parr correlation functional (B3LYP) method with 6-31G** basis set [19-22].

2.5 Phosphomolybdate Total Antioxidant Capacity Assay

The total antioxidant capacities (TAC) of the Schiff bases were evaluated by phosphomolybdenum assay using the method described by Pierre and coworkers [23] while ascorbic acid was used as the standard. 1.0 mL of reagent (0.6 M sulphuric acid, 28 µM sodium phosphate and 4 µM ammonium molybdate) was reacted with a fractional part of the solution of the compounds (1.0 mL of 1000 µg). The covered tubes were incubated at 95 ^{o}C in a water bath for 90 minutes after which the samples were cooled to room temperature and a UV spectrophotometer was used to measure the absorbance of the aqueous solution of each at 695 nm. The procedure was repeated for a blank solution containing 1.0 mL of reagent solution. The TAC studies were performed three times and the mean was expressed as equivalents of ascorbic acid.

3. RESULTS AND DISCUSSION

3.1 Characterization of the Schiff bases

I (N-(5-methoxysalicylidene)anline) = $C_{14}H_{13}NO_2$, Molecular weight: 227.26 g/mol, Yield: 74%, IR (cm^{-1}): 3200-2500 (O−H), 1616 (C=N), 1565-1447 (C=C), 1272 (C−O). ^{1}H NMR (ppm): 12.36 (s, 1H, OH), 8.90 (s, 1H, C=N), 7.40-6.80 (m, 6H, C−H_{Ar}), 3.70 (s, 3H, C−$H_{methoxy}$). ^{13}C NMR (ppm): 163.60, 154.83, 152.40, 148.88, 130.02, 129.34, 127.45, 121.86, 121.04, 119.69, 118.01, 115.66, 114.38, 56.07. UV: 308 (n−π*), 367 (π−π*). Elemental analysis in %: Found (Calculated): 74.01 (73.99), 5.79 (5.77), 6.15 (6.16).

II (N-(5-methoxysalicylidene)-4-chloroanline) = $C_{14}H_{12}ClNO_2$, Molecular weight: 261.70 g/mol, Yield 80%, IR (cm^{-1}): 3300-2550 (O−H), 1617 (C=N), 1591-1488 (C=C), 12721(C−O). ^{1}H NMR (ppm): 13.00 (s, 1H, OH), 8.90 (s, 1H, C=N), 7.40-6.70 (m, 5H, C−H_{Ar}), 3.37 (s, 3H, C−$H_{methoxy}$). ^{13}C NMR (ppm): 163.86, 154.89, 152.41, 148.90, 131.07, 129.67, 127.14, 121.57, 121.01, 119.35, 118.01, 115.79, 114.05, 56.29. UV: 313 (n−π*), 371 (π−π*). Elemental analysis in %: Found (Calculated): 64.23 (64.25), 4.58 (4.62), 5.38 (5.35).

III (N-(5-methoxysalicylidene)-2-methyl-5-chloroanline) = $C_{15}H_{14}ClNO_2$, Molecular weight: 275.73 g/mol, Yield 84%, IR (cm^{-1}): 3300-2400 (O−H), 1614 (C=N), 1564-1487 (C=C), 1270 (C−O). ^{1}H NMR (ppm): 12.33 (s, 1H, OH), 8.84 (s, 1H, C=N**)**, 7.37-6.86 (m, 6H, C−H_{Ar}), 3.71 (s, 3H, C−$H_{methoxy}$), 2.25 (s, 3H, C−H_{methyl}). ^{13}C NMR (ppm): 164.39, 154.99, 152.43, 149.02, 132.50, 131.79, 126.71, 121.43, 118.54, 118.03, 115.85, 113.33, 110.69, 55.95, 17.38. UV: 320 (n−π*), 372 (π−π*). Elemental analysis in %: Found (Calculated): 65.35 (65.34), 5.15 (5.12), 5.10 (5.08).

The Schiff bases were obtained in good yields as solids. They were stable in air and soluble in most organic solvents but insoluble in water. They were of different shades of yellow. The IR spectra results of the compounds confirmed the formation of the azomethine bonds ν(−HC=N). All the compounds exhibited the azomethine absorption bands in the range 1617-1614 cm^{-1}. They displayed the phenolic stretching ν(C−O) vibrations at 1272-1270 cm^{-1} and the hydroxyl (O−H) absorption bands around 3640-3630 cm^{-1}. The compounds showed the aromatic (C=C) bands in the range 1591-1447 cm^{-1} [18, 24-28].

The ^{1}H NMR spectra data of the compounds (Figs. 1-3) revealed a singlet signal at δ 13.00-12.33 ppm assigned to the phenolic –OH protons. All the compounds showed a singlet signal at δ 8.91-8.85 ppm attributed to the azomethine (−HC=N) protons which further confirmed the formation of the Schiff bases [18, 24, 25, 27]. The aromatic protons appeared as multiplets at δ 7.40-6.70 ppm [18, 26-28]. A sharp singlet signal attributed to the methoxy groups' protons appeared at δ 3.70, 3.37 and 3.71 ppm in the spectra of the compounds **I**, **II** and **III** respectively while the signal at 2.25 ppm in compound **III** was assigned to the protons of the methyl group [18, 24-27, 29]. The ^{13}C NMR spectra of the compounds (Figs. 4-6) were consistent with the ^{1}H NMR. All of the ^{13}C NMR spectra showed the azomethine carbon peaks in the range 164.39-163.60 ppm and the aromatic carbon around 154.99-110.69 ppm. The carbon of the methoxy groups were displayed at δ 56.07, 56.29 and 55.95 ppm for the compounds **I**, **II** and **III** respectively. Furthermore, the carbon peak of the methyl group in compound **III** appeared at δ 17.38 ppm [18, 28]. The UV spectra of the compounds showed two absorption peaks at 270-320 nm and 367-372 nm which were assigned to n-π* of the azomethines and π-π*of the aromatic rings in the compounds [18].

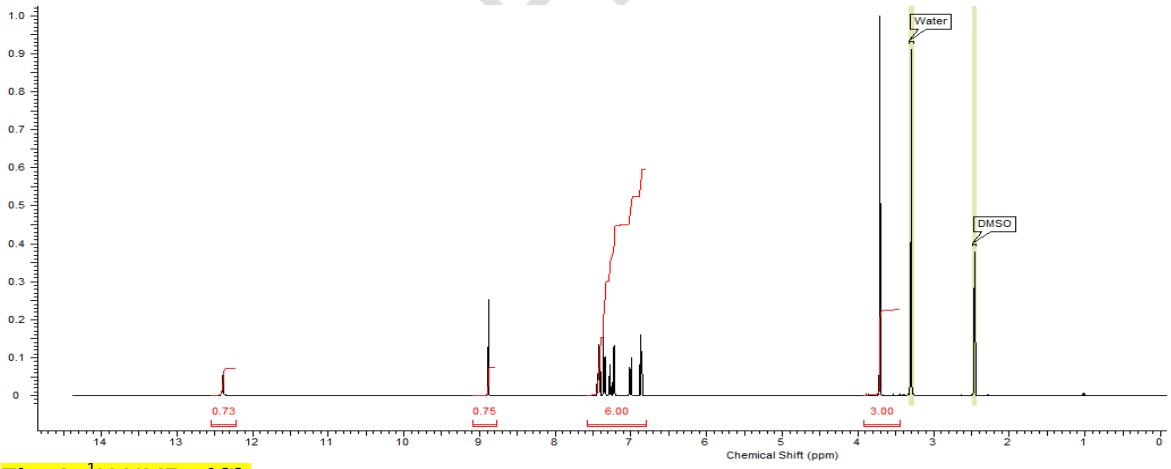

Fig. 1: ^{1}H NMR of [I].

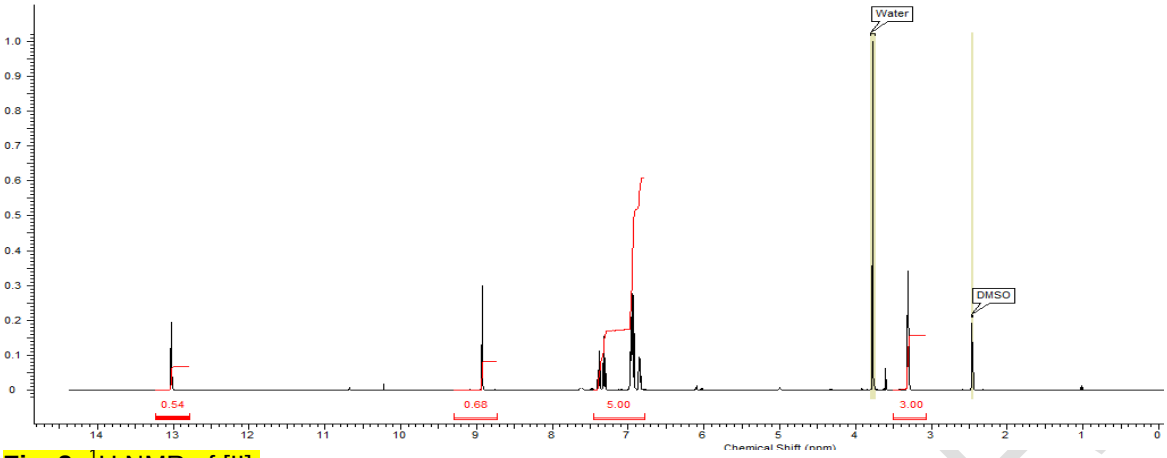

Fig. 2: ^{1}H NMR of [II].

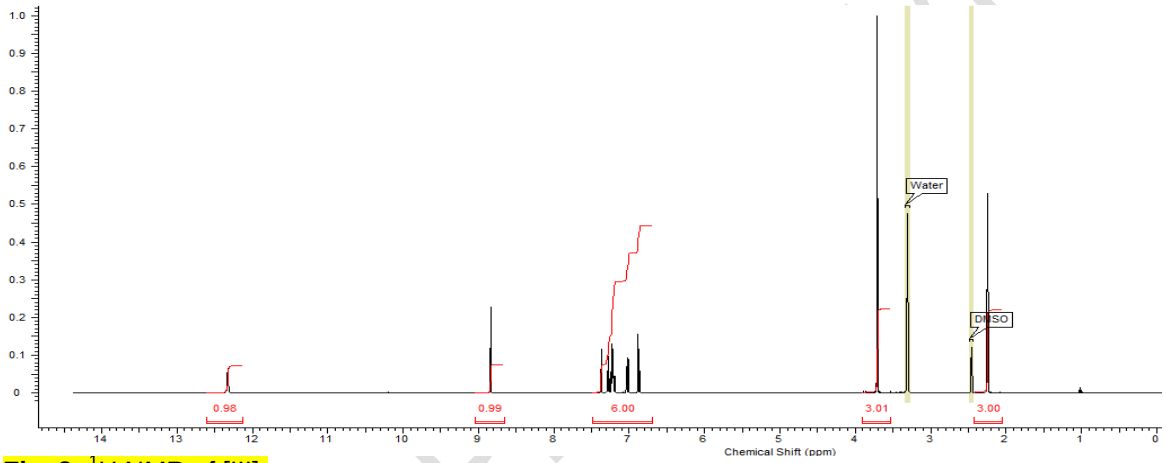

Fig. 3: ^{1}H NMR of [III].

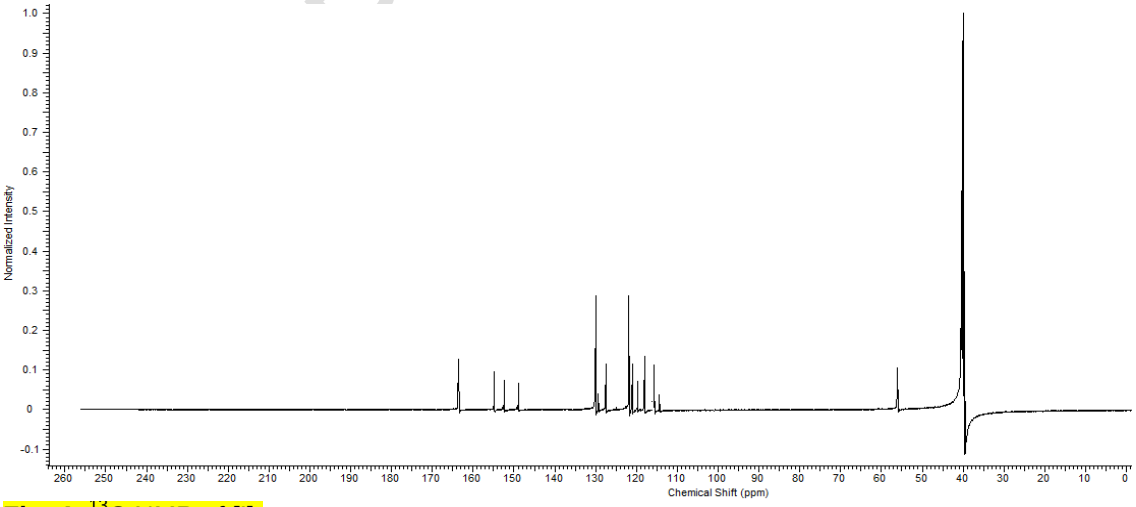

Fig. 4: ^{13}C NMR of [I].

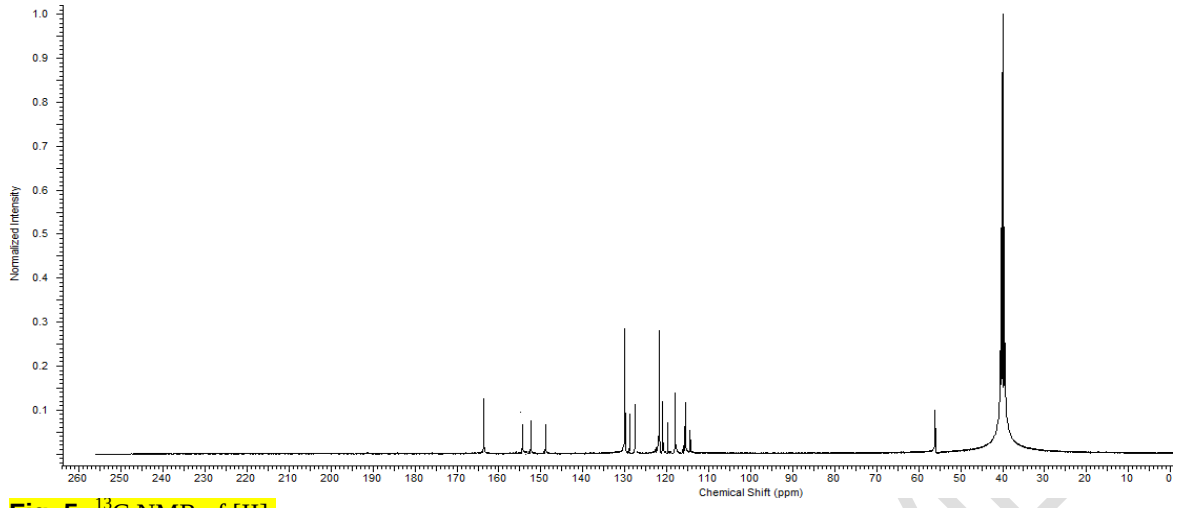

Fig. 5: ^{13}C NMR of [II].

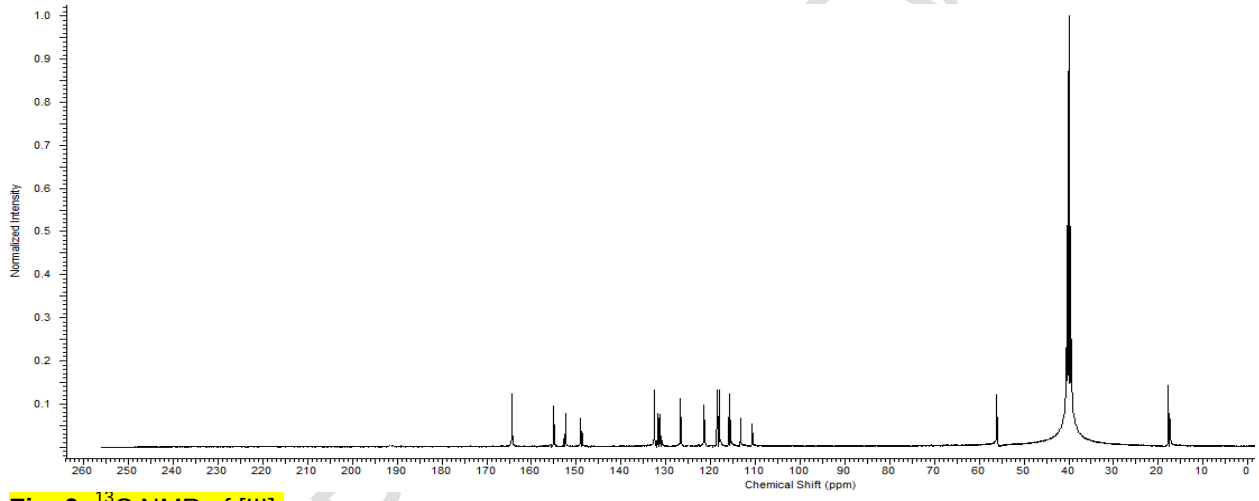

Fig. 6: ^{13}C NMR of [III].

3.2 Computational Studies

3.2.1 Theoretical IR Spectra

The theoretical IR vibrational frequency data of the Schiff bases presented in Table 1 and Figs (7-9) were in agreement with the experimental data. The absorption bands of the azomethine protons (−HC=N) in the Schiff bases appeared at 1687, 1686 and 1676 cm^{-1} for compounds **I, II** and **III** in the theoretical spectra while the experimental values were observed at 1616, 1617 and 1614 respectively. The phenolic (C−O) stretching vibrations of the compounds were displayed around 1337-1335 cm^{-1} theoretically while the experimental spectra showed the bands around 1272-1270 cm^{-1}. However, the ν(O−H) absorption bands in the compounds ranged from 3268-3238 cm^{-1} in the theoretical data while the experimental values were observed in the range 3300-2400 cm^{-1}. The

theoretical spectra showed the aromatic (C=C) absorption bands in the range 1655-1426 cm^{-1} while the experimental data were observed around 1592-1442 cm^{-1}.

Compounds	IR (cm^{-1})				UV-Vis (nm)
	OH	C=N	C=C	C−O	
I	3242	1687	1655-1447	1337	237, 254, 262, 340
II	3268	1686	1647-1440	1335	239, 250, 268, 345
III	3238	1676	1644-1426	1337	251, 262, 288, 317, 375

Table 1: Theoretical IR data of the Schiff bases

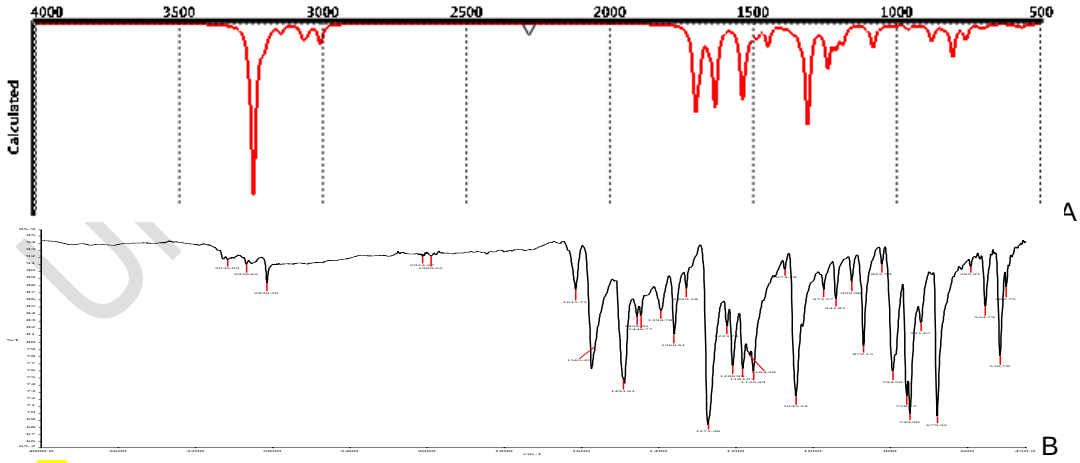

Fig. 7: IR spectra of compound **I**, theoretical (A) and experimental (B)**.**

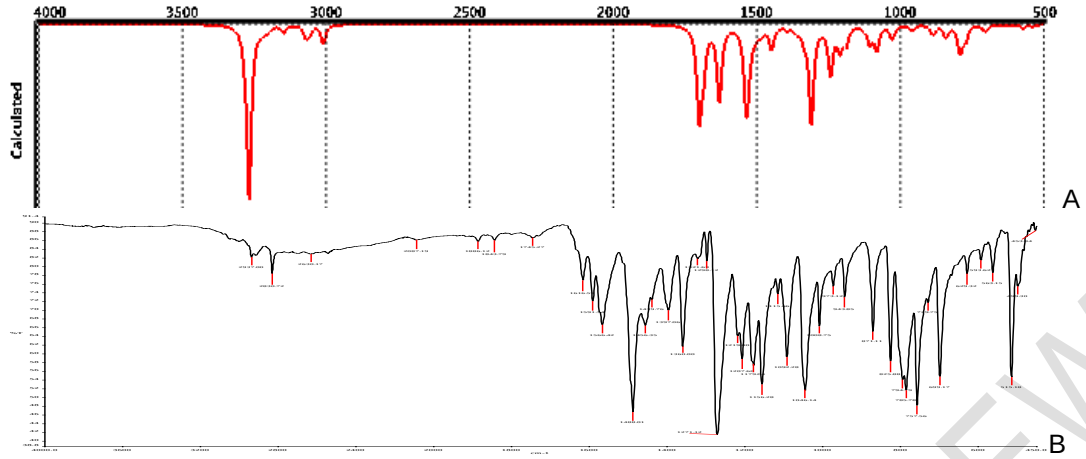

Fig. 8: IR spectra of compound **II**, theoretical (A) and experimental (B)**.**

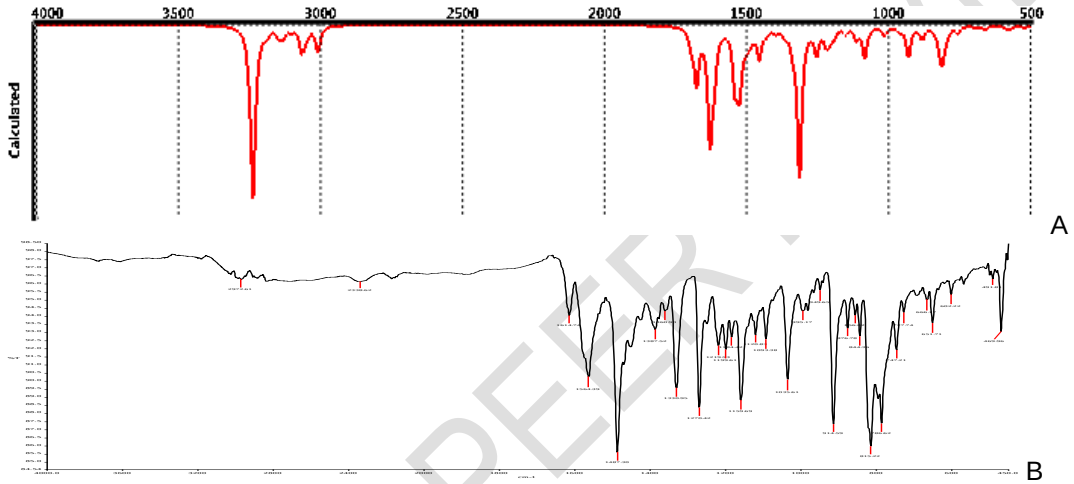

Fig. 9: IR spectra of compound **III**, theoretical (A) and experimental (B)**.**

3.2.2 Theoretical NMR Spectra

The theoretical chemical shifts of the compounds (Table 2) were comparable to the experimental values. The data obtained revealed that the aromatic hydrogen in compound **I**: H6, H11, H14, H1, H10, H15, H13, H17 appeared at 7.74, 7.79, 7.90, 7.89, 8.38, 8.20, 8.38, 7.89 ppm respectively in the theoretical study, these ranged at 7.40-6.80 ppm in the experimental spectrum. The azomethine (HC=N, H4) and hydroxyl (−OH, H9) hydrogen were observed at 9.19 ppm and 13.07 ppm in the theoretical spectrum while they appeared experimentally at 8.90 ppm and 12.36 ppm respectively. The

three hydrogen (H2, H3, H5) of the methoxy group appeared at 4.68 ppm in the theoretical study and 3.70 ppm experimentally. The aromatic carbon in compound **I** ranged at 151.43-110.92 ppm in the theoretical calculations, these appeared experimentally in the range 154.83-114.38 ppm. Moreover,

Positions of	δ (ppm)		
H & C	**I**	**II**	**III**
H1	7.89	7.82	7.87
C1	144.80	145.01	145.09
H2	4.68	4.68	4.70
C2	116.35	116.44	116.43

the azomethine and methoxy carbon were observed at 160.41 ppm and 52.39 ppm in the theoretical spectrum, these appeared at 163.60 ppm and 56.07 ppm respectively in the experimental study. Nevertheless in compound **II**, the aromatic hydrogen: H6, H11, H14, H1, H10, H13, H17 were observed at 7.73, 7.80, 7.91, 7.82, 8.23, 8.23, 7.82 ppm respectively in the theoretical calculations. These ranged at 7.40-6.70 ppm in the experimental spectrum. The hydrogen of the azomethine (−HC=N, H4) and hydroxyl (–OH, H9) groups were observed at 9.14 ppm and 12.84 ppm in the theoretical spectrum while they appeared at 8.90 ppm and 13.00 ppm respectively in the experimental study. The three hydrogen (H2, H3, H5) of the methoxy group appeared at 4.68 ppm in the theoretical study and 3.37 ppm experimentally. Furthermore, the aromatic carbon in compound **II** ranged at 151.44-111.46 ppm in the

H3	4.68	4.68	3.21
C3	115.31	115.02	116.02
H4	9.19	9.14	9.30
C4	151.43	151.44	151.74
H5	4.68	4.68	3.21
C5	113.13	113.30	113.11
H6	7.74	7.73	7.84
C6	110.92	111.46	111.41
H7	-	-	3.21
C7	160.41	161.11	159.62
H8	-	-	8.04
C8	147.99	146.66	145.36
H9	13.07	12.84	13.60
C9	114.84	116.12	113.79
H10	8.38	8.23	4.70
C10	123.20	123.83	137.53
H11	7.79	7.80	7.81
C11	118.63	134.39	121.11
H12	-	-	4.70
C12	123.20	123.82	126.29
H13	8.38	8.23	8.15
C13	114.84	116.12	127.77
H14	7.90	8.23	7.91
C14	52.39	52.41	20.10
H15	8.20	-	-
C15	-	-	52.41
H16	-	-	-
C16	-	-	-
H17	7.89	-	-
C17	-	-	-

Table 2: Theoretical NMR data of the compounds

theoretical calculations, these appeared experimentally in the range 154.33-114.05 ppm. The azomethine and methoxy carbon appeared at 161.11 ppm and 52.41 ppm theoretically and at 163.86 ppm and 56.29 ppm respectively in the experimental data. However, the aromatic hydrogen in compound **III**: H6, H11, H14, H1, H8, H13 appeared at 7.84, 7.81, 7.91, 7.87, 8.04, 8.15 ppm respectively in the theoretical data, these ranged at 7.37-6.86 ppm in the experimental study. The hydrogen of the azomethine (−HC=N, H4) and hydroxyl (–OH, H9) groups appeared at 9.30 ppm and 13.60 ppm in the theoretical spectrum while they were experimentally observed at 8.84 ppm and 12.33 ppm respectively. The chemical shifts of the three hydrogen of the methoxy (H2, H10, H12) and methyl (H3, H5, H7) groups were observed at 4.70 ppm and 3.21 ppm in the theoretical calculations while they appeared at 3.71 ppm and 2.25 ppm respectively in the experimental data. The aromatic carbon in compound **III** ranged at 151.74-111.41 ppm in the theoretical calculations, these appeared experimentally in the range 154.99-110.69 ppm. The carbon in the azomethine appeared at 159.62 ppm in the theoretical spectrum and was observed at 164.39 ppm in the experimental study. Moreover, the methoxy and methyl groups' carbon appeared at 52.41 ppm and 20.10 ppm theoretically while they were displayed at 55.95 ppm and 17.38 ppm respectively in the experimental spectrum.

3.2.3 Theoretical Electronic Spectra

The theoretical electronic spectra values of the compounds were in agreement with the experimental data. The agreement between the theoretical and experimental electronic spectra data supported the proposed structures. The theoretical spectrum of compound **I** revealed four absorption bands at 237, 254, 262 and 341 nm, these bands were related to the promotion of electrons from HOMO – 2 → LUMO, HOMO → LUMO + 1, HOMO – 3 → LUMO + 1 and HOMO → LUMO respectively. Similarly, compound **II** exhibited four absorption bands at 239, 250, 268 and 345 nm. These bands were obtained when electrons were promoted from HOMO – 2 → LUMO, HOMO – 3 → LUMO, HOMO → LUMO + 1, HOMO – 1→ LUMO and HOMO → LUMO respectively. However, compound **III** displayed six absorption bands at 251, 262, 263, 289, 317 and 375 nm. These bands were related to the promotion of electrons from HOMO → LUMO + 2, HOMO – 3 → LUMO, HOMO → LUMO + 1, HOMO – 2→ LUMO, HOMO – 1 → LUMO and HOMO → LUMO respectively.

3.2.4 Frontier Molecular Orbitals

The highest occupied molecular orbital (HOMO) and the lowest unoccupied molecular orbital (LUMO) are also called the frontier molecular orbitals. They govern the way molecules relate with other species. The HOMO is the orbital of highest energy containing electrons, thus, donates electrons while LUMO is the orbital of lowest energy. According to the frontier molecular orbital theory, the energy gap between the HOMO and LUMO is anticipated to play fundamental roles in the intra- and inter- charge transfers. The energy band gaps between the HOMO and LUMO is more significant in considering electronic transitions than individual orbital components of a molecule. Since the difference between the LUMO and HOMO shows the reactivities and stabilities of molecules in chemical reactions. Therefore, the lower the energy gap, the more reactive and less stable the molecule [20, 30, 31]. Thus, Fig. 10 displays the proposed structures, optimized structures, HOMO and LUMO of the synthesized Schiff bases while the calculated energy band gaps for compounds **I, II** and **III** are presented in Table 3 as 3.9, 3.9 and 3.6 eV respectively. This indicates that compound **III** is expected to be more reactive than compounds **I** and **II**. Thus, compounds **I** and **II** would be more stable than compound **III**.

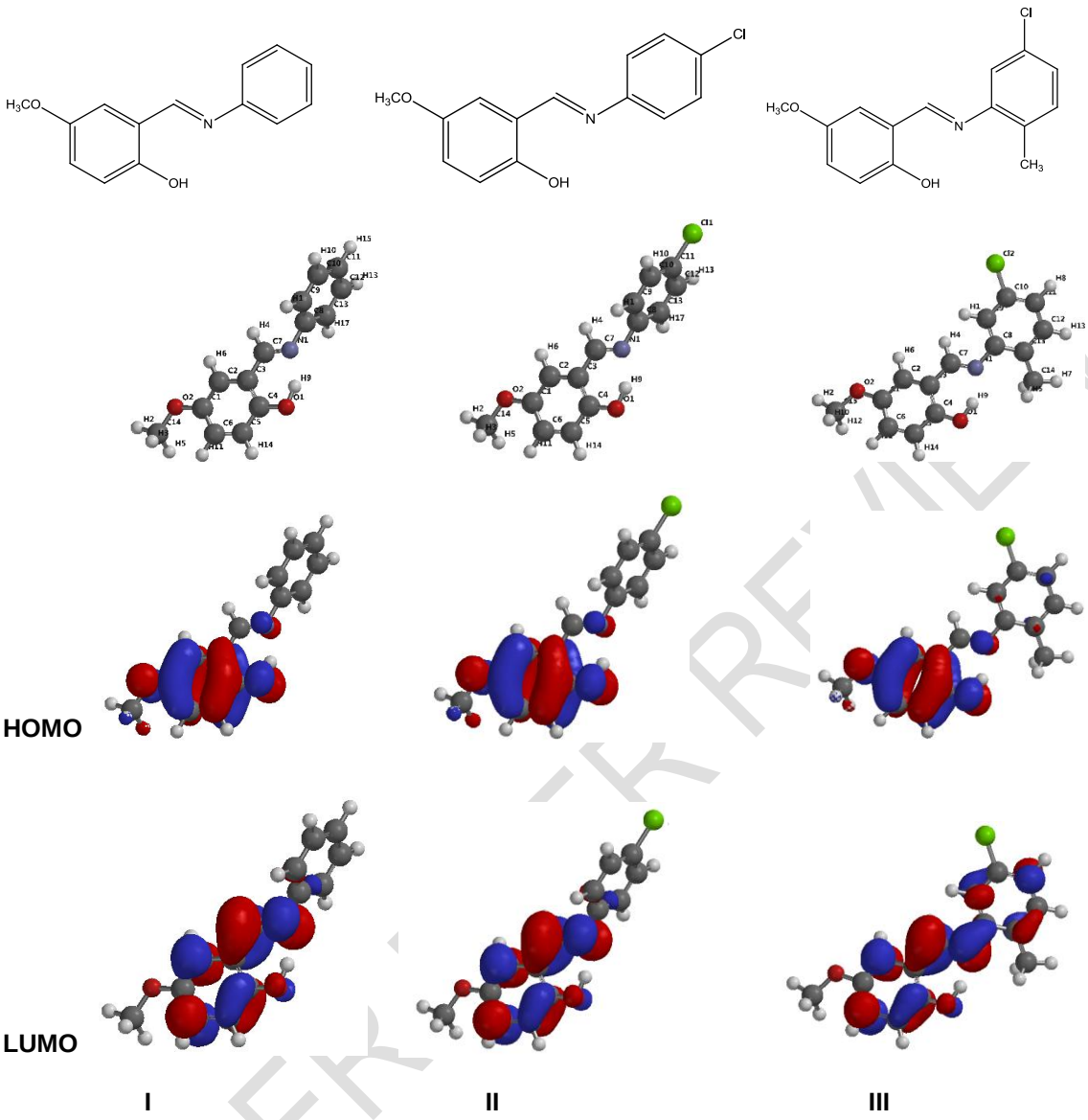

Fig. 10: Proposed structures, Optimized structures, HOMO and LUMO of the compound.

	I	II	III
HOMO	-5.4	-5.5	-5.5
LUMO	-1.5	-1.6	-1.9
ENERGY GAPS	3.9	3.9	3.6

Table 3: The HOMO, LUMO and Energy gap of the compounds

3.3 Total Antioxidant Capacity

The total antioxidant capacities results (TAC) of the synthesized compounds are presented in Table 4. The results revealed that all the synthesized compounds exhibited antioxidant activities. This showed that they have the ability to inhibit or limit the harm caused by free radicals. Antioxidants function by freely giving out electrons to free radicals without changing into electron–scavenging substances themselves [32, 33]. They are chemicals that deter or lessen the damage caused by free

radicals and can also be called free radical scavengers [34-36]. Free radicals are molecules that have one or more unpaired electrons. They are unstable and very reactive because of the unpaired electrons. In an attempt to be stable, free radicals either give out or receive electrons from another molecules which then become free radicals [35, 37]. These new free radicals will either give out or receive electrons from another molecules, consequently, commencing chain reactions. If free radicals are too many in a biological system, they can overpower the cells' usual defenses. Hence, causing harms to the cells which ultimately lead to many diseases [33, 34]. On the other hand, if there are antioxidants in the cells, they donate electrons to the free radicals, thus, making them become stable and ending the chain reactions [38].

The differences observed in the TAC of the Schiff bases are due to the presence of various substituents on the compounds and possibly the positions of the substituents. Compound **II** showed the highest total antioxidant capacities while compound **I** displayed the least capacities. Hence, compound **II** would be a better free radical scavenger.

Compounds	TAC µg per AA
I	0.50
II	0.65
III	0.62

Table 4: The total antioxidant capacity of the salicylaldimines

*Key: AA = ascorbic acid

4. CONCLUSION

A comparison of the theoretical and experimental data revealed that the theoretical values were in agreement with the experimental results, therefore, supporting the suggested structures. The calculated energy gaps indicated that compound **III** would be more reactive than compounds **I** and **II**. The TAC results showed that compound **II** displayed the highest antioxidant capacities, which consequently implies that it has the highest capability to impede or lessen the harm caused by free radicals.

COMPETING INTERESTS DISCLAIMER:

Author has declared that no competing interest exist. The products used for this research are commonly and predominantly use products in her area of research and country. There is absolutely no conflict of interest between the author and producers of the products because the products are not intended to be used as avenues for any litigation but for the advancement of knowledge. Also, the research was not funded by the producing company rather it was funded by Organization of Women in Science in Developing World and personal efforts of the author.

REFERENCES

1. Kalaivani S, Priya NP, Arumachalam S. Schiff bases : facile synthesis, spectral characterization and biocidal studies. Int J Appl Biol Pharm. 2012;3:219-23.

2. Gupta V, Singh S, Gupta YK. Synthesis and Antimicrobial Activity of some Salicylaldehyde Schiff bases of 2-aminopyridine. Res J Chem Sci. 2013;3(9):26-9.
3. Dueke-Eze CU, Fasina TM, Idika N. Synthesis, electronic spectra and inhibitory study of some Salicylaldehyde Schiff bases of 2-aminopyridine. Afr. J. Pure Appl. Chem. 2011;5(2):13-8.
4. Zayed EM, Zayed MA. Synthesis of novel Schiff's bases of highly potential biological activities and their structure investigation. Spectrochim. Acta A Mol. Biomol. Spectrosc. 2015;143:81-90.
5. Fasina TM, Dada RO. Substituent effect on electronic absorption and biological properties of Schiff bases derived from aniline. J Chem Pharm Res. 2013;5(10):177-81.
6. Hossain MS, Banu LA, E-Zahan MK, Haque MM. Synthesis, Characterization and Biological Activity Studies of Mixed Ligand Complexes with Schiff base and 2,2'-Bipyridine. Int. J. Appl. Sci. 2019;6(1:2):1-7.
7. Khan MI, Khan A, Hussain I, Khan MA, Gul S, Iqbal M, et al. Spectral, XRD, SEM and biological properties of new mononuclear Schiff base transition metal complexes. Inorg. Chem. Commun. 2013;35:104-9.
8. Sathe BS, Jaychandran E, Jagtap VA, Sreenivasa GM. Synthesis characterization and anti-inflammatory evaluation of new fluorobenzothiazole Schiff bases. Int. j. pharm. res. dev. 2011;3(3):164-9.
9. Sondhi SM, Singh N, Kumar A, Lozach O, Meijer L. Synthesis, anti-inflammatory, Analgesic and kinase (CDK-1, CDK-5, and GSK-3) inhibition activity evaluation of Benzimidazole/benzoxazole derivatives and some Schiff's bases. Bioorg. Chem. 2006;14(11):3758-6.
10. Chaubey AK, Pandeya SN. Synthesis and anticonvulsant activity (Chemo Shock) of Schiff and Mannich bases of Isatin derivatives with 2-Amino pyridine (mechanism of action). Int. J. Pharmtech Res. 2012;4(4):590-8.
11. Hasan MA, Kumari N, Singh K, Mishra L. Mixed ligand complexes of Cu(II)/Zn(II) ions containing (m-)/(p-) carboxylato phenyl azo pentane 2,4-dione and 2,2-bipyridine/1,10 phenanthroline: Synthesis, characterization, DNA binding, nuclease and topoisomerase I inhibitory activity. Spectrochim. Acta A Mol. Biomol. Spectrosc. 2016;152:208-17.
12. Kasumov VT, Sahin O, Aktas HG. Synthesis, characterization, crystal structure, redox-reactivity and antiproliferative activity studies of Cu(II) and Pd(II) complexes with F, CF_3 bearing 3,5-di- tert-butylsalicylaldimines. Polyhedron. 2016;115:119-27.
13. Ghosh AK, Mitra M, Fathima A, Yadav H, Choudhury AR, Nair BU, et al. Antibacterial and catecholase activities of Co(III) and Ni(II) Schiff base complexes. Polyhedron. 2016;107:1-8.
14. Devi J, Batra N. Synthesis, characterization and antimicrobial activities of mixed ligand transition metal complexes with isatin monohydrazone Schiff base ligands and heterocyclic nitrogen base. Spectrochim. Acta A Mol. Biomol. Spectrosc. 2015;135:710-9.
15. Belal AAM, El-Deen IM, Farid NY, Rosan Z, Refat MS. Synthesis, spectroscopic, coordination and biological activities of some transition metal complexes containing ONO tridentate Schiff base ligand. Spectrochim. Acta A Mol. Biomol. Spectrosc. 2015;149:771-89.
16. Avaji PG, Vinod KCH, Patil SA, Shivananda KN, Nagaraju C. Synthesis, spectral characterization, in-vitro microbiological evaluation and cytotoxic of novel macrocyclic bis hydrazine. Eur. J. Med. Chem. 2009;44(9):3552-9.
17. Abu-Dief AM, Mohamed IMA. A review on versatile applications of transition metal complexes incorporating Schiff bases. Beni-Seuf Univ. J. Appl. 2015;4(2):119-33.
18. Demehin AI, Babajide JO, Salihu SO, Sabejeje AJ. Synthesis, Spectroscopic and Inhibitory Study of Some Substituted Schiff Bases. IJIRAS. 2017;4(2):411-3.
19. Paul MK, Singh YD, Singh NB, Sarkar U. Emissive bis-salicylaldiminato Schiff base ligands and their zinc(II) complexes: Synthesis, photophysical properties, mesomorphism and DFT studies. J. Mol. Struct. 2015;1081:316-28.
20. Semire B, Mutiu OA, Oyebamiji AK. DFT and *AB INITIO* Methods on NMR, IR and Reactivity Indices of Indol-3-Carboxylate and Indazole-3-Carboxylate Derivates of Cannabinoids: Comparative Study. J. Phys. Chem. 2017;13(4):353-77.
21. Shajari N, Yahyaei H. Spectroscopic and DFT Investigation on Some New Aryl (trichloroacetyl)carbamate Derivates. Phys. Chem. Res. 2020;8(4):705-18.

22. Ikram M, Rehman S, Khan A, Baker RJ, Hofer TS, F.Subhan, et al. Sythesis, characterization, antioxidant and selective xanthine oxidase inhibitory studies of transition metal complexes of novel amino acid bearing Schiff base ligand. Inorganica Chim. Acta. 2015;428:117-26.
23. Pierre BK, Pierre SH, Tatjana S. Study of Polyphenol Content and Antioxidant Capacity of *Myrianthus Arboreus* (Cecropiaceae) Root Bark Extracts. Antioxidants 2015;4:410-26.
24. Demehin AI, Oladipo MA, Semire B. Synthesis, Spectroscopic, Antibacterial and Antioxidant Activities of Pd(II) Mixed-Ligand Complexes Containing Tridentate Schiff Bases. Egypt. J. Chem. 2019;62:423-6.
25. Demehin AI, Oladipo MA, Semire B. Synthesis, spectroscopic, biological activities and DFT calculations of nickel(II) mixed-ligand complexes of tridentate Schiff bases. Ecletica Quim J. 2020;45(1):18-43.
26. Abo-Aly MM, Salem AM, Sayed MA, Aziz AAA. Spectroscopic and structural studies of the Schiff base 3-methoxy-N-salicylidene-o-amino phenol complexes with some transition metal ions and their antibacterial, antifungal activities. Spectrochim. Acta A Mol. Biomol. Spectrosc. 2015;136:993-1000.
27. Ananda KS, Yiheyis BZ, Nithyakalyani D. Synthesis, Structural Characterization, Corrosion inhibition and invitro antimicrobial studies of 2-(5-Methoxy-2-Hydroxybenzylideneamino) Phenol Schiff Base Ligand and its transition metal complexes. Int. J. Chemtech Res. 2014;6(11):4569-78.
28. Oloyede-Akinsulere AI, Babajide JO, Salihu SO. Synthesis, Antibacterial and Antioxidant Activities of Some Tridentate Substituted Salicylaldimines. Asian J. Appl. Chem. Res. 2018;1(4):1-10.
29. Thangadurai AS, Johnpeter MP, Manikandan R, Raj AP. Synthesis, Spectral Characterization and Biological Evaluation of Schiff Base Derived From 3-Methoxy Salicylaldehyde with Aniline and Its Transition Metals. Int J Sci Technol Res. 2020;9(3).
30. Annaraj B, Pan S, Neelakantan MA, Chattaraj PK. DFT study on the ground state and excited state intramolecular proton transfer of propargyl arm containing Schiff bases in solution and gas Phases. Comput. Theor. Chem. 2014;1028:19-26.
31. Tabrizi L, Chiniforoshan H, Tavakol H. New mixed palladium(II) complexes based on the antiepileptic drug sodium valproate and bioactive nitrogen-donor ligands: Synthesis, structural characterization, binding interactions with DNA and BSA, *in vitro* cytotoxicity studies and DFT calculations. Spectrochim. Acta A Mol. Biomol. Spectrosc. 2015;141:16-26.
32. Ibrahim M, Khan A, Ikram M, Rehman S, Shah M, Nabi HH, et al. In Vitro Antioxidant Properties of Novel Schiff Base Complexes. Asian J. Chem. Sci. 2017;2:1–12.
33. Suleman M, Khan A, Baqi A, Kakar MS, Samiullah, Ayub M. Antioxidants, its role in preventing free radicals and infectious diseases in human body. Pure appl. biol. 2018;7:380-8
34. Sayed SS, Shah D, Ibrahim K, Sajjad A, Umar A, Atiq ur R. Synthesis and Antioxidant Activities of Schiff Bases and Their Complexes: An Updated Review. Pure appl. biol. 2020; 10(6): 6936 - 63.
35. Uddin MN, Khandaker S, Moniruzzaman, Amin MS, Shumi W, Rahman MA, et al. Synthesis, Characterization, Molecular modeling, Antioxidant and Microbial Properties of some Titanium(IV) complexes of Schiff Bases. J. Mol. Struct. 2018;1166:79-90.
36. Al Zoubi W, Al-Hamdani AAS, Kaseem M. Synthesis and antioxidant activities of Schiff bases and their complexes: a review. Appl. Organomet. Chem. 2016;30:810-7.
37. Neelofar, N. Ali, A. Khan, S. Amir, N. A. Khan, M. Bilal. Synthesis of schiff bases derived from 2- hydroxy-1-naphthaldehyde and their Tin(Ⅱ) complexes for antimicrobial and antioxidant activities. Bull Chem Soc Ethiop. 2017;31(3):445-56.
38. Zehiroglu C, Sarikaya SBO. The importance of antioxidants and place in today's scientific and technological studies. J. Food Sci. Technol. 2019;56(11):4757–74.